

Ultrafast electronic motion in hydrogen molecular ions induced by a high power intense laser

H. Mineo^{a,b,*}, Y. Teranishi^{b,c}, S.D. Chao^a, S.H. Lin^{b,c}

^a Institute of Applied Mechanics, National Taiwan University, Taipei 106, Taiwan, ROC

^b Institute of Atomic and Molecular Sciences, Academia Sinica, P.O. Box 23-166, Taipei 106, Taiwan, ROC

^c Institute of Applied Chemistry, Institute of Molecular Science, Chiao-Tung University, Hsin-Chu, Taiwan, ROC

ARTICLE INFO

Article history:

Received 26 April 2010

In final form 10 September 2010

Available online 17 September 2010

ABSTRACT

In this Letter we report a method for controlling electronic localization in a molecular ion, on an attosecond time scale, using a high-intensity laser, based on two different excitation mechanisms. One takes place during ionization, and the other takes place sequentially, following ionization. The electronic excited states of the hydrogen molecular ion are created during ionization by taking the configuration interaction mixing of neutral molecules into account. We detect the ultrafast oscillatory electronic motion between two atoms in a hydrogen molecular ion occurring due to the creation of excited states during the course of ionization.

© 2010 Elsevier B.V. All rights reserved.

1. Introduction

The behaviors of the molecules in a high power laser have been extensively studied, both theoretically and experimentally. Such work has looked at photoionization and dissociation [1–7], Coulomb explosions [8], and high harmonic generation [7,9]. Compared to other molecular dynamical processes, molecular excitation has received less attention, both theoretically and experimentally, because the excitation probabilities of the molecules are considered to be too small to affect their dynamical processes. This is due to the fact that the typical frequency of a high power laser is much smaller than that of electronic motion, leading to adiabatic behavior. However, excitation might play important roles in various molecular electronic and dynamical processes [10–14]. For example, it is well known that the electronic excitation of neutral molecules enhances ionization rates significantly [10,15]. Another example may be the photodissociation process of molecules in an intense femtosecond pulsed laser. According to recent experiments involving mass spectra [3,10], the observed fragmentation yields of molecular ions M^+ can be larger than expected, this is as per our calculations carried out using the Keldysh–Faisal–Reiss (KFR) theory [16–18] combined with the RRKM theory [3,19]. This fragment enhancement may be explained by taking electronic excitations into account, since the creation of an electronically excited ion may open new fragmentation channels.

Recently, Palacios et al. [12,13] studied the excitation and ionization of hydrogen molecules in an ultra-short VUV laser pulse by solving the time-dependent Schrödinger equation, including the vibrational degrees of freedom. Their results showed that Rabi-type oscillation is induced, which is not accessible by direct photon absorption. Teranishi et al. [14] and Gibson et al. [20–23] have studied high multiphoton excitation, where Gibson et al. have assumed nearly degenerated final states so that the dynamical Stark shift is negligibly small. Teranishi et al. have assumed that the first excitation energy is much larger than both the photon energy and the transition energy between excited states. Excited states are strongly coupled with each other by the photon and these Editors found that a collective excitation takes place in which the excitation probability of every excited state is almost a linear function of intensity on a log–log plot, and the slope is independent of the final state. The results agree well with the recent experiments performed by Kong et al. [24,25]. Markevitch et al. [10] calculated the total fragmentation fraction of polyatomic molecular ions via a sequential non-adiabatic electronic excitation model. The strong laser field merges all of the electronic states into a quasi-continuum, or QC. The non-adiabatic transition from ground to continuum excitations, through a doorway (charge-transfer) state, induces multi-electron polarization, leading to dissociative ionization within pulse duration. This model can qualitatively reproduce the experimental data reflecting dissociative ionization in large molecules. However, since this model consists of three elements, namely, the photofragmentation of neutral molecules, a multi-electronic distribution, and dissociative ionization, it is difficult to check its validity solely by measuring the dependence of the laser field on intensity, wavelength and pulse duration. Recent experiments have demonstrated a new approach for controlling

* Corresponding author at: Institute of Applied Mechanics, National Taiwan University, Taipei 106, Taiwan, ROC.

E-mail addresses: mineo@gate.sinica.edu.tw (H. Mineo), tera@mail.nctu.edu.tw (Y. Teranishi).

the electron localization in a D₂ molecule, using the attosecond pulse train (APT) and a many-cycle infrared pulse [26], where the APT is synthesized using both even and odd high-order harmonics with an IR field. Researchers have also performed a numerical simulation by solving the time-dependent Schrödinger equation, determining that the excitation will take place after a long propagation along the internuclear distance, with an IR pulse, inducing the asymmetric ejection of the deuterium ions. The maximum asymmetry is estimated to be approximately 2%, both theoretically and based on experimental results.

Our aim in this Letter is to study possible mechanisms for the creation of electronically excited ions and for the control of electron localization in molecular ions, on an attosecond time scale. Here we consider two excitation mechanisms; one takes place during the ionization process, while the other takes place sequentially, following the ionization. The ground-state wave function of a neutral molecule has small components stemming from doubly excited configurations. If an electron is removed from said doubly excited configurations, the resultant ion is naturally in an excited state. This is the excitation mechanism that takes place during the course of ionization, which is expected to occur more evidently for molecules having larger doubly excited components in ground state. The adiabatic DC Stark mixing mechanism, on the other hand, takes place after the ionization of a neutral molecule. Since ionization takes place predominantly when the laser intensity is maximum, the ionized molecules are still in the laser field, which induces the excitations of the ions. When the field oscillation is sufficiently slow relative to the electronic motion, the electronic wave function exhibits a form of oscillatory motion following the adiabatic eigenstates, under a static DC electric field, which can be regarded as a type of (de-)excitation. Since this excitation probability returns to zero when the laser is turned off, we refer to it as field-driven (or temporal) (de-)excitation, due to the adiabatic DC Stark mixing. This kind of excitation may be hard to observe. However, it is expected that the use of the attosecond laser as a probe enables us to observe the ultrafast motion of electronic wave packets [27,28]. It should be noted that these attosecond dynamics are induced by the substantially longer duration of the interaction (i.e., the femtosecond laser).

In this Letter, we use a hydrogen molecule as an example. The electronic wave-packet motion of a hydrogen molecular ion [27,28], due to the excitation during the ionization, is calculated under fixed nuclei and strong field approximations. We find that an ultrafast oscillation of an electron cloud between two hydrogen atoms, even though it is subsequent to the ionization, oscillates with the frequency of the laser, due to the field-driven DC Stark mixing.

This paper is organized as follows. In Section 2, we introduce the theoretical methods of calculating parameters of the molecular ionization process and the excitation mechanisms of molecular ions. Here we consider the different excitation mechanisms: excitation during ionization and field-driven DC Stark mixing. The excitation during ionization is calculated by taking the CI mixing of molecules into account. In Section 3, we show the numerical results and present a discussion of the time-dependent excited state populations and electronic wave-packet motion, as calculated based on the different excitation mechanisms. In Section 4, we conclude and summarize this work.

2. Theoretical methods

2.1. The generalized KFR theory for molecules with CI

As shown in the introduction, ionization stemming from a doubly excited component results in the production of an excited ion.

The probability of this process can be calculated with the use of the generalized KFR theory [16] with the initial wave function having a doubly excited configuration. In this subsection, the mathematical details of the basic formulation are presented. The electronic excited states are characterized by nuclear repulsive potential, and electronic motion is affected by nuclear motion. Throughout the paper we assume that nuclear motion is negligible (fixed nuclei approximation), because the excitation mechanisms considered in this work occur within a short period of time (a few fs).

Here we consider the single ionization of a neutral molecule in ground state, which exhibits a wave function, given by $\psi_M(r, R)$. Due to the irradiation of the laser field, $\vec{F}(t) = -\frac{d}{dt}\vec{A}(t) = \vec{F} \cos \omega t$, an electron is emitted with varying momentum, \vec{p} , leading to the production of molecular ions, both in ground and excited states. Throughout the remainder of this paper we have used atomic units.

The total wave function of a molecule in the intense laser field is given by:

$$\Psi_M(r, R, t) = \psi_M(r, R) \exp(-iE_g t) + \Psi_M^+(r, R, t), \quad (1a)$$

$$\Psi_M^+(r, R, t) = \int \frac{d^3 p}{(2\pi)^3} c_g(\vec{p}, t) \psi_{M^+}^g(\vec{p}, r, R, t) + \sum_{\alpha} \int \frac{d^3 p}{(2\pi)^3} c_{\alpha}(\vec{p}, t) \psi_{M^+}^{\alpha}(\vec{p}, r, R, t), \quad (1b)$$

where E_g is the ground-state energy of a neutral molecule, r denotes the electron spin and coordinates, R denotes the nuclear coordinates, $\psi_{M^+}^g(\vec{p}, r, R, t)$ ($\psi_{M^+}^{\alpha}(\vec{p}, r, R, t)$) are the electronic wave functions of the molecular ion in the excited state, α (in the ground state, g), with the ionized electron having momentum \vec{p} . Here, the coefficients, $c_{\alpha}(\vec{p}, t)$, neglecting the Coulomb potential, $c_g(\vec{p}, t)$, are calculated perturbatively as follows:

$$c_k(\vec{p}, t) = -i \int_{-\infty}^t dt' \langle \psi_{M^+}^k(\vec{p}, r, R, t') | \hat{V}(p_1 \cdots p_{N_e}, t') | \psi_M \exp(-iE_g t') \rangle, \quad (2a)$$

$$\hat{V}(p_1 \cdots p_{N_e}, t') = \sum_{i=1}^{N_e} \left(\frac{e p_i \cdot \vec{A}(t)}{m} + \frac{e^2 A(t)^2}{2m} \right), \quad (2b)$$

with $k = g, \alpha$. Here, the velocity gauge is adopted for the interaction Hamiltonian, in KFR theory.

The neutral-state wave function with doubly excited configuration is described by the linear combinations of Slater determinants, as follows:

$$\psi_M(r, R) = (c_g |\phi_1^+(1)\phi_1^-(2)\phi_2^+(3)\phi_2^-(4)\cdots\phi_H^+(N_e-1)\phi_H^-(N_e)| + \sum_{ab} c_{ab} |\phi_1^+(1)\phi_1^-(2)\phi_2^+(3)\phi_2^-(4)\cdots\phi_a^*\cdots\phi_b^*\cdots\phi_H^+(N_e-1)\phi_H^-(N_e)|), \quad (3a)$$

$$\phi_k(i) = \sum_j b_{kj}^M \chi_j(i), \quad (3b)$$

where N_e is the number of electrons, b_{kj}^M are the molecular ion orbital coefficients for the j^{th} nucleus, the subscript D represents a doubly excited configuration, H is the highest molecular orbital (HOMO), and c_g and c_{ab} are the CI coefficients of the ground and doubly excited configurations, respectively. We note that in Eq. (3a) arbitrary two orbitals in the Slater determinant, in the second line, are replaced by the excitation configurations ϕ_a^* and ϕ_b^* , where the Slater determinant in the first line is considered as a reference. The ionized-state wave function is given by the following:

$$\psi_{M^+}^k(\vec{p}, r, R, t) = \exp(-iE_k t) \frac{1}{\sqrt{2}} \left(|\Phi_1^+(1)\Phi_1^-(2)\Phi_2^+(3)\Phi_2^-(4)\cdots\Phi_p^+(N_e-1)\Phi_H^-(N_e)| - |\Phi_1^+(1)\Phi_1^-(2)\Phi_2^+(3)\Phi_2^-(4)\cdots\Phi_H^+(N_e-1)\Phi_p^-(N_e)| \right), \quad (4a)$$

$$\Phi_k(i) = \sum_j b_{kj}^{M^+} \chi_j(i), \quad (4b)$$

$$\Phi_p(i) = \exp \left[i(\vec{p} \cdot \vec{r}_i - \frac{1}{2m_e} \int_0^t dt' (\vec{p} + e\vec{A}(t'))^2) \right], \quad (4c)$$

where $b_{kj}^{M^+}$ are the molecular ion orbital coefficients for the j th nucleus and ϕ_p is the Volkov wave function in the velocity gauge [17,18]. As discussed in our previous papers [5–7], it is reasonable to assume that the ionization predominantly takes place with the HOMOs. The atomic orbitals (AOs), χ_j , are therefore given by the AOs of the hydrogen atom.

Using a generalized Bessel function, the populations of the ground and singly excited states of molecular ions at $t = T = 2\pi/\omega$ can be calculated as follows [3,6]:

$$|C_k|^2 = \int \frac{d^3p}{(2\pi)^3} |c_k(\vec{p}, T)|^2, \quad (5a)$$

$$c_k(\vec{p}, T) = 2\pi i \sqrt{2} c_k \left(\sum_j b_{kj}^{M^+} \chi_j(\vec{p}) \exp(-i\vec{p} \cdot \vec{R}_j) \right) \left(\frac{p^2}{2m_e} + I_p \right) \times \sum_N J_N^* \left(V_p, \frac{U}{2\omega}, \zeta = 0 \right) \delta \left(\frac{p^2}{2m_e} + I_p + U - N\omega \right), \quad (5b)$$

with $V_p = \frac{e\vec{E} \cdot \vec{p}}{m_e \omega^2}$, $U = \frac{e^2 E^2}{4m_e \omega^2}$, and c_k ($k = g, \alpha$) representing the CI coefficient, where $k = g$ represents the ground state and $k = \alpha = 1, \dots, N_s$ are the N_s excited states.

The electronic wave-packet motion is defined as follows:

$$\int dz |\Psi_M^+(r, R, t)|^2 = \int dz \int \frac{d\phi_p d\cos\theta_p dp^2}{(2\pi)^3} |c_g(\vec{p}, t) \psi_{M^+}^g(\vec{p}, r, R, t) + \sum_\alpha c_\alpha(\vec{p}, t) \psi_{M^+}^\alpha(\vec{p}, r, R, t)|^2, \quad (6)$$

where the molecular axis is taken as the z -axis, the origin (0 0 0) is at the center of the hydrogen atoms, and θ_p is measured from the z -axis. Since time-dependent electronic motion in a hydrogen molecular ion is dependent on the momentum of the ionized electron of the molecule, in this work we observe the electronic wave-packet motion by fixing the direction of the ionized, outgoing electron at the molecular axis, and plot $\int dz \frac{d}{d\cos\theta_p} |\Psi_M^+(r, R, t)|^2$.

2.2. DC Stark shift

In this subsection, we present the calculation of the electronic excitations, which takes place following the ionization. If the field oscillation is slow compared to the electronic motion, the resulting excited states adiabatically change under the static DC field. This field driven (temporal) (de-)excitation probability is calculated by taking the adiabatic DC Stark mixing into account. The adiabatic energy levels of molecular ions are given by diagonalizing the energy matrix under the slowly oscillating electric field given by

$$\langle \psi_i | \hat{H}_0 + \hat{V}(t) | \psi_j \rangle = E_i \delta_{ij} - \langle \psi_i | \vec{\mu} \cdot \vec{E}(t) | \psi_j \rangle, \quad (7)$$

where ψ_i are the unperturbed states, $\vec{\mu}$ is the dipole moment operator, the indices $i, j = 0, \dots, N_s$, and E_i expresses the ground ($i = 0$) and excitation ($i, j = 0, \dots, N_s$) state energies, without the laser field. The eigenenergies, $\varepsilon^{(k)}$, and eigenvectors, $\varphi^{(k)}$, are defined as the eigenvalues and eigenvectors obtained by diagonalizing the energy matrix in Eq. (7). The total wave function is given by the superposition of $\varphi^{(k)}$ as follows:

$$\Psi(r, t) = \sum_{k=0}^{N_s} a_k \varphi^{(k)}(r, t). \quad (8)$$

The coefficients, a_k , are determined by assuming that the molecular ion is in the ground state at $t = 0$ (i.e., $\langle \psi_i | \psi_i \Psi(r, 0) \Psi(r, 0) \rangle = \sum_{k=0}^{N_s} a_k \langle \psi_i | \psi_i \varphi^{(k)}(r, 0) \varphi^{(k)}(r, 0) \rangle = \delta_{i0}$). The coefficients, a_k , are assumed to be time-independent under the slowly oscillating laser field.

Populations of the states, ψ_l ($l = 0, \dots, N_s$), are given by

$$P_l = |\langle \psi_l | \Psi(r, t) \rangle|^2. \quad (9)$$

As mentioned in the introduction, to perform a comparison of the electronic wave-packet motion induced by different excitation mechanisms, we define the electronic density distribution of molecular ions. The electronic density, $\rho(x, y)$, projected onto the (x, y) plane is defined by

$$\rho(x, y) = \int_{-\infty}^{\infty} dz |\Psi(r, t)|^2. \quad (10)$$

3. Numerical results and discussion

In this section, we show the numerical results pertaining to the population of electronic excited states and the electronic wave-packet motion for a hydrogen molecule. The internuclear distance of a neutral hydrogen molecule, $R = 1.4$ a.u., is taken from a database [29], while the ground-state energy and probability of the doubly excited configuration of a neutral molecule are calculated via the CID method. The ground and excited states of the molecular ion are calculated via the CIS method. The above calculations are performed using the GAUSSIAN03 program [30]. Under fixed nuclei approximation, the geometry of a molecular ion is the same as that of a neutral molecule. 6-31G+(d, p) basis sets are used throughout these calculations. Here, we assume a linearly polarized laser along the molecular axis.

According to the calculated CI coefficients of the neutral hydrogen molecule, the ground state of the neutral hydrogen molecule contains the ground ($\sim 98.8\%$) and a doubly excited ($\sim 1.2\%$) configurations, while the contribution from other configurations is negligible. The calculated vertical ionization potential is $I_p = 15.36$ eV. The first excitation energy of a molecular ion, H_2^+ , is given by $E(D_1) = 18.52$ eV at the equilibrium nuclear distance, $R = 1.4$ a.u., of the neutral molecule (H_2). It should be noted that the transition dipole moments between the ground and excited states, which are higher than the first excitation, are negligible (i.e., $|\vec{\mu}_{0i}| \ll |\vec{\mu}_{01}|$ ($i > 1$)). Therefore, our system can be regarded as a two-energy-level

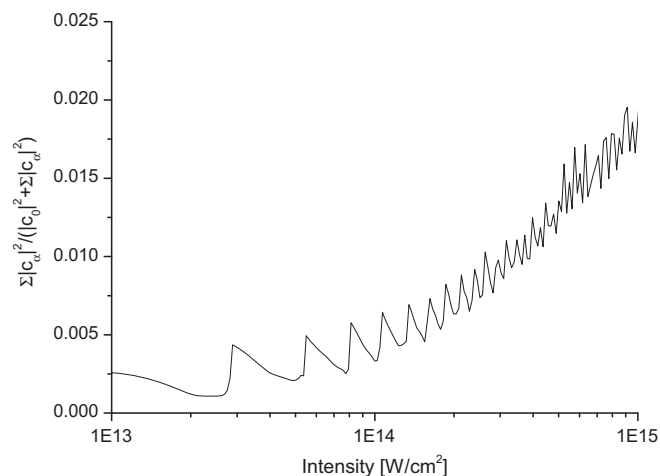


Figure 1. Excited state populations obtained during the ionization of a neutral hydrogen molecule, taking CI mixing into account, plotted as a function of laser intensity. The wavelength of the laser is fixed at $\lambda = 800$ nm.

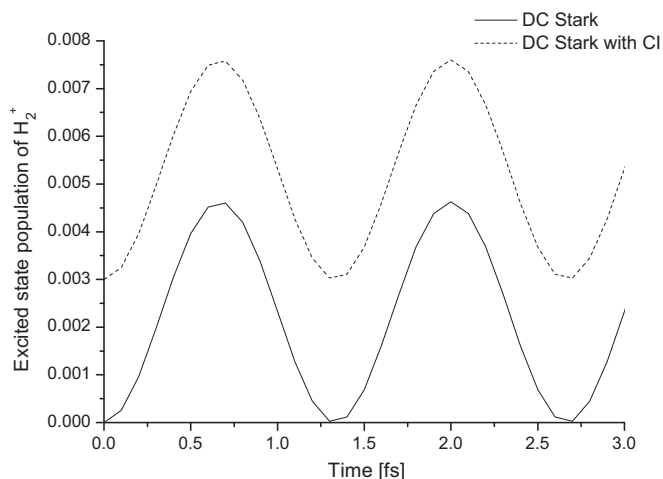


Figure 2. First excited state populations of H_2^+ at a laser intensity $I = 10^{14}$ W/cm 2 and a wavelength $\lambda = 800$ nm, plotted as a function of time. The solid (dashed) curve shows an excited state population calculated by DC Stark (DC Stark and CI) mixing.

system, and a doubly excited configuration can be regarded as two electrons in the first excited state.

In Figure 1, we plot the laser intensity dependence of the excitation probability of a molecular ion created following the ionization of a neutral hydrogen molecule in the configuration mixed ground state (see Eq. (5)). Here, and in what follows, the laser wavelength, λ , is assumed to be $\lambda = 800$ nm. For the calculation of the electronic excited-state probability of a molecular ion, at time $t = T = 2\pi/\omega = 2.67$ fs, where ω is the laser frequency, we use the generalized KFR theory for the photoionization process. As we find in the figure, the curve shows a number of small oscillations, which usually appear in a photoionization rate constant as a function of the laser intensity, calculated using the KFR or Keldysh theory. This is due to the different behavior exhibited at each absorbed photon number. The curve increases slowly with increasing laser intensity, beginning from 0.25% at an intensity of $I = 10^{13}$ W/cm 2 and

approaching 1.8% at $I = 10^{15}$ W/cm 2 . We can see in Figure 3a that the observation of the time dependence of the wave-packet motion caused by the CI mixings can be continued, where the probability of an electronic excited state is less than 1%. Thus, a CI mixing mechanism works reasonably well for inducing electronic wave-packet motion in a hydrogen molecular ion. Since KFR or Keldysh theories are strong field theories and Coulomb interaction is treated as a perturbation, the laser intensity should be strong enough to ionize the neutral molecule. In the case of a H_2 molecule, $I > \sim 3 \times 10^{13}$ W/cm 2 gives a rate constant of $W > 10^{-9}$ s $^{-1}$, therefore it is reasonable to apply the KFR or Keldysh theory at a range of intensity, I , greater than 10^{13} W/cm 2 .

In Figure 2, the first excited-state probability at the laser intensity $I = 10^{14}$ W/cm 2 is plotted as a function of time. The solid and dashed lines show the probability calculated by taking the DC Stark and the DC Stark and CI mixing into account, respectively. Here we assume that at $t = 0$ there is no electric field (i.e., a laser field $\vec{F}(t) = \vec{F} \sin(\omega t)$ is used). In this figure, we find that CI mixing increases the population of excited state electrons independent of time. We also find that the degree of increase can be estimated by taking into account the excitation during ionization (0.33%), which is comparable in magnitude to that obtained in the case of the adiabatic DC Stark mixing (0.55%). Both curves show slow oscillation with a periodicity of $T/2 = \pi/\omega = 1.33$ fs, which is equivalent to a half cycle of the laser field.

In Figures 3a and b, we plot the time-dependent electronic wave-packet motion of a hydrogen molecular ion, calculated (a) through the excitation mechanism during the course of ionization by taking the CI mixing into account, and (b) due to both adiabatic DC Stark and CI mixings. Here, the laser intensity is fixed at $I = 10^{14}$ W/cm 2 and the wavelength is $\lambda = 800$ nm. We also note that, in (a), the laser field is switched off after the ionization, while in (b) the laser field is present during and after the ionization. In Figure 3a, the excited states are populated during the ionization of a neutral hydrogen molecule due to the CI mixing, subsequently the electronic excited state population of the hydrogen molecular ion following ionization is approximately 0.33%. Here, we fix the direction of the ionized outgoing electron momentum toward

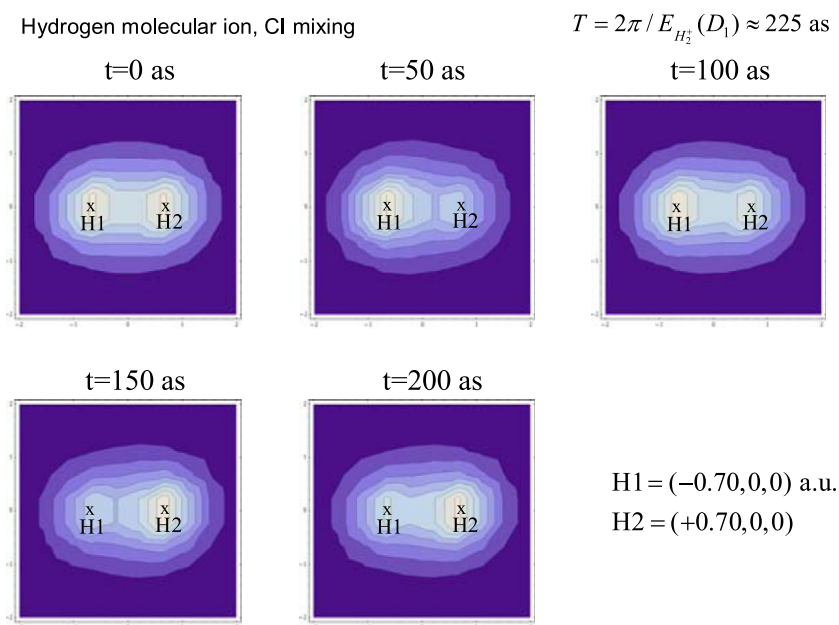


Figure 3a. Electron distributions of H_2^+ with excitation during ionization, taking CI mixing into account. We note that, before the ionization ($t < 0$), the laser intensity is $I = 10^{14}$ W/cm 2 and the wavelength is $\lambda = 800$ nm, and that, at $t = 0$, the laser field is switched off. Here, we fix the direction of the ionized outgoing electron momentum toward the positive x-axis. The height of the peak is 0.15, which is divided into 10 equally spaced contour lines.

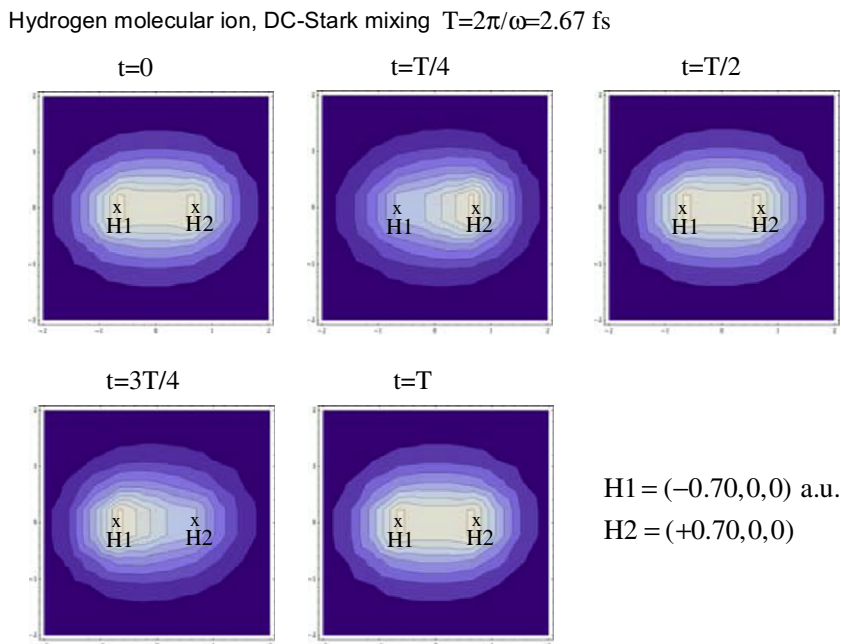


Figure 3b. Electron distributions of H_2^+ with excitations populated by field-driven DC Stark mixing at a laser intensity of $I = 10^{14}$ W/cm² and a wavelength of $\lambda = 800$ nm. Similarly to Fig. 3a, we fix the direction of the ionized outgoing electron momentum toward the positive x -axis, and the height of the peak is 0.15, which is divided into 10 equally spaced contour lines.

positive x . At $t=0$, the electrons are distributed symmetrically about the vertical axis, and the two peaks are concentrated on H atoms. As time progresses, the electron cloud begins to move toward the left, and oscillates between two hydrogen atoms with an approximate periodicity of $t = 2\pi/E_{H_2^+}(D_1) = 225$ as, which is much smaller than the time period of the oscillation of the laser field. If the ionized outgoing electron momentum tends toward negative x , the electron cloud begins to shift toward positive x . In Figure 3b, it is shown that the electronic excited states are populated, during the course of ionization; this is due to adiabatic DC Stark mixing. We should note here that the initial electron distribution at $t=0$ depends on the relative phase of the coefficients, c_0 and c_1 , and that the direction that the electron cloud moves in depends solely on the factor of the time dependence of the laser field, $\vec{F}(t)$. Here, we assume that, at $t=0$, the electron clouds are symmetrically distributed about the vertical axis, and that the coefficients are consequently determined to be $c_0 = 0.998$ and $c_1 = \pm 0.057i$, where the magnitudes, $|c_0|^2 = 0.9967$ and $|c_1|^2 = 0.0033$, are obtained from the excited state population during the course of ionization, which is caused by the CI mixing. As time progresses, the electron cloud moves toward the right, and at $t = T/2 = 1.33$ fs it returns to its original distribution, before moving toward the left at $t = 3T/4$. Finally, following an optical cycle, the electron cloud returns to the original distribution as at $t=0$, due to its adiabaticity. The periodicity of the oscillation of the electron cloud between two atoms is $T = 2\pi/\omega = 2.67$ fs. It seems that, in the presence of the laser field, the motion of the electron clouds is almost the same despite the inclusion of the CI mixing. It should be noted that for both Figures 3a and b, we have used an identical scale for the contour plot (i.e., the height of the peak is 0.15, which is divided into 10, equally spaced contour lines).

4. Summary and conclusions

In this work we have calculated the electronic wave-packet motion in a hydrogen molecular ion by considering two different electronic excitation mechanisms. One takes place during the course of

ionization, while the other takes place sequentially, after ionization. For a description of the molecular wave function and calculation of the photoionization rate constant, we use the KFR theory; a strong field approximation theory.

By including the CI mixing in the ground state of a hydrogen molecule, the excited state is created during the ionization process. In spite of the fact that, after ionization, the population of excited state is estimated to be 0.33%, which appears to be a very small quantity, we have still succeeded in inducing ultrafast electronic motion by switching off the laser following ionization. In our case, relative to the periodicity of the laser $T = 2.67$ fs, the periodicity of the electronic oscillation between H atoms is $T = 225$ as, which is roughly 1/10 the length of the periodicity of the oscillating laser and oscillation induced by DC Stark mixing. Following ionization, the DC Stark mixing creates the excited states, and the excitation probability changes adiabatically under the driven field. Electronic motion under DC Stark mixing follows the oscillating field, and its maximum probability is 0.45%, which is comparable to that created by CI mixing (0.33%). Although a H_2 molecule is the most trivial case for a discussion of CI mixing, it is expected that the contribution to excitation probability in a larger molecule would be much larger, due to the number of electron correlations. For example, in the case of O_2 and N_2 molecules, excited state probabilities in the neutral molecules are estimated in KFR theory, at a laser intensity $I = 10^{14}$ W/cm² and a wavelength of $\lambda = 800$ nm to be roughly 4%; more than 3 times that of a hydrogen molecule. The ejection asymmetry of D_2^+ [26] is roughly estimated to be 2%, both theoretically and experimentally, which is larger than that obtained in our calculations. If we take CI mixing, at a large nuclear distance (~ 4 a.u.), into account, double configuration reaches $\sim 24\%$ in a neutral H_2 molecule. Although the excited state population is somehow expected to be reduced during ionization, CI mixing may still induce a non-negligible contribution to a localization in the electron density, and to electron movement between the two hydrogen atoms, at a velocity corresponding to the inverse of the energy gap, which is also observed in the ejection asymmetry of D_2^+ [26].

We expect that our approach, based on excitation during ionization, can be applied to larger molecule systems, which enables us to discuss electronic motion in ions, and to present a quantitative discussion of the fragmentation patterns, and the angular and momentum distributions. Although we have not discussed the dissociation of molecular ions in this Letter, for large molecular ions we expect that the number of fragments produced from excitation during ionization is comparable to the total number of fragments.

Acknowledgement

The Editors thank Academia Sinica of the Republic of China, and the National Science Council.

References

- [1] H. Harada, S. Shimizu, T. Yatsuhashi, S. Sakabe, Y. Izawa, N. Nakashima, *Chem. Phys. Lett.* 342 (2001) 563.
- [2] N. Nakashima, S. Shimizu, T. Yatsuhashi, S. Sakabe, Y. Izawa, *J. Photochem. Photobiol., C* 1 (2000) 131.
- [3] Qiaoqiao Wang et al., *J. Phys. Chem. C* 113 (2009) 11805.
- [4] M. Sharifi et al., *J. Phys. Chem. A* 111 (2007) 9405.
- [5] K. Mishima, M. Hayashi, J. Yi, S. Chin, H.L. Selzle, E.W. Schlag, *Phys. Rev. A* 66 (2002) 033401.
- [6] H. Mineo, K. Nagaya, M. Hayashi, S.H. Lin, *J. Phys. B* 40 (2007) 2435.
- [7] H. Mineo, S.D. Chao, K. Nagaya, K. Mishima, M. Hayashi, S.H. Lin, *Chem. Phys. Lett.* 439 (2007) 224.
- [8] L.J. Frasinski, K. Codling, P.A. Hatherly, *Science* 246 (1989) 1029.
- [9] P. Agostini, L.F. Dimauro, *Rep. Prog. Phys.* 67 (2004) 813.
- [10] A.N. Markevitch, D.A. Romanov, S.M. Smith, H.B. Schlegel, M.Y. Ivanov, R.J. Levis, *Phys. Rev. A* 69 (2004) 013401.
- [11] A.S. Alnaser, M. Zamkov, X.M. Tong, C.M. Maharjan, P. Ranitovic, C.L. Cocke, I.V. Litvinyuk, *Phys. Rev. A* 72 (2005) 041402.
- [12] A. Palacios, H. Bachau, F. Martín, *Phys. Rev. A* 75 (2007) 013408.
- [13] A. Palacios, H. Bachau, F. Martín, *Phys. Rev. A* 74 (2006) 031402.
- [14] Y. Teranishi, M. Hayashi, F. Kong, S.L. Chin, S.D. Chao, H. Mineo, S.H. Lin, *Mol. Phys.* 333 (2008) 106.
- [15] I. Kawata, H. Kono, Y. Fujimura, A.D. Bandrauk, *Phys. Rev. A* 62 (2000) 031401.
- [16] L.V. Keldysh sov, *Phys. JETP* 20 (1965) 1307.
- [17] F.H.M. Faisal, *J. Phys. B* 6 (1973) L89.
- [18] H.R. Reiss, *Phys. Rev. A* 22 (1980) 1786.
- [19] H. Eyring, S.H. Lin, S.M. Lin, *Basic Chemical Kinetics*, Wiley, New York, 1980.
- [20] G.N. Gibson, *Phys. Rev. Lett.* 89 (2002) 263001.
- [21] G.N. Gibson, *Phys. Rev. A* 67 (2003) 043401.
- [22] R.N. Coffee, G.N. Gibson, *Phys. Rev. A* 69 (2004) 053407.
- [23] G.N. Gibson, L. Fang, B. Moser, *Phys. Rev. A* 74 (2006) 041401.
- [24] F. Kong, Q. Luo, H. Xu, M. Sharifi, D. Song, S.L. Chin, *J. Chem. Phys.* 125 (2006) 133320.
- [25] D. Song, A. Azarm, Y. Kamali, K. Liu, A. Xia, Y. Teranishi, S.H. Lin, F. Kong, S.L. Chin, *J. Phys. Chem. A* 114 (2010) 3087.
- [26] K.P. Singh et al., *Phys. Rev. Lett.* 104 (2010) 023001.
- [27] M. Kanno, T. Kato, H. Kono, Y. Fujimura, F.H.M. Faisal, *Phys. Rev. A* 72 (2005) 033418.
- [28] K. Hatumiya, H. Kono, Y. Fujimura, I. Kawata, A.D. Bandrauk, *Phys. Rev. A* 66 (2002) 04303.
- [29] NIST Chemistry WebBook, (<http://webbook.nist.gov/chemistry/>).
- [30] G.W.T.M.J. Frisch et al., T.Keith, GAUSSIAN, Inc., Pittsburgh, 2003.